Inorganic Chemistry
Article

*Inorg. Chem.* **2010**, *49*, 10907–10913 **10907**
DOI: 10.1021/ic101749g

# $Ca_9Lu(PO_4)_7:Eu^{2+},Mn^{2+}$: A Potential Single-Phased White-Light-Emitting Phosphor Suitable for White-Light-Emitting Diodes

**Ning Guo,[†,‡] Yeju Huang,[†,‡] Hongpeng You,*[,†] Mei Yang,[†,‡] Yanhua Song,[†,‡] Kai Liu,[†,‡] and Yuhua Zheng[†,‡]**

[†]*State Key Laboratory of Rare Earth Resource Utilization, Changchun Institute of Applied Chemistry, Chinese Academy of Sciences, Changchun 130022, People's Republic of China, and* [‡]*Graduate University of the Chinese Academy of Sciences, Beijing 100049, People's Republic of China*

Received June 25, 2010

A novel white-light-emitting phosphor $Ca_9Lu(PO_4)_7:Eu^{2+},Mn^{2+}$ has been prepared by solid-state reaction. The photoluminescence properties indicate that there is an efficient energy transfer from the $Eu^{2+}$ to $Mn^{2+}$ ions via a dipole−quadrupole reaction. The obtained phosphor exhibits a strong excitation band between 250 and 430 nm, matching well with the dominant emission band of a UV light-emitting-diode (LED) chip. Upon excitation of UV light, white light is realized by combining a broad blue-green emission band at 480 nm and a red emission band at 645 nm attributed to the $Eu^{2+}$ and $Mn^{2+}$ ions. The energy-transfer efficiency and critical distance were also calculated. Furthermore, the phosphors can generate lights from blue-green through white and eventually to red by properly tuning the relative ratio of the $Eu^{2+}$ to $Mn^{2+}$ ions through the principle of energy transfer. Preliminary studies showed that the phosphor might be promising as a single-phased white-light-emitting phosphor for a UV white-light LED.

## 1. Introduction

As a commercially available solid-state source for general lighting sources, light-emitting diodes (LEDs) could play a significant role in reducing global energy consumption. White-light LEDs are attracting significant attention as one of the most promising general illumination sources because they can offer benefits such as high brightness, long lifetime, small size, low power consumption, and environmentally friendly characteristics.[1−4] The present strategy for producing white light is to combine a GaN-based blue LED chip with $Y_3Al_5O_{12}:Ce^{3+}$ (YAG:Ce) yellow phosphor. However, warm white-light illumination usually cannot be achieved by this approach because of the red deficiency of the spectral emission in this LED system. This drawback has limited the possible applications of white-light LEDs, such as uses in the medical and architectural lighting fields.[5,6] Another approach might solve this problem by using a UV LED chip coated with three emitting blue, green, and red phosphors to generate warm white light.[7] This approach provides white-light LEDs with excellent color rendering indexes. However, in this white-light LED system, the blue emission efficiency is poor because of the strong reabsorption of the blue light by the green and red phosphors.[8] Therefore, it is urgent to develop a single-phased white-light-emitting phosphor that can be effectively excited by UV light to enhance the luminous efficiency and color rendering index. More importantly, compared to the multiple emitting components of the white-light LED system, the single-phased white-light-emitting phosphor for a UV-pumped white-light LED would enable easy fabrication with perfect stability and color reproducibility.[9,10]

It is well-known that the emission and excitation spectra of $Eu^{2+}$ ions usually consist of broad bands due to transitions between the $4f^7$ ground state and the crystal-field components of the $4f^65d$ excited-state configuration. The emission of $Mn^{2+}$ ions varies from green to red, depending on the influence of the crystal field.[11] Owing to the forbidden $^4T_1-{}^6A_1$ transition of $Mn^{2+}$ ions, the emission intensity of a $Mn^{2+}$-ion singly doped phosphor is low under UV excitation. From the above-mentioned considerations, it is necessary to enhance the emission intensity of $Mn^{2+}$-doped materials by introducing an efficient sensitizer $Eu^{2+}$. Moreover, white light can be obtained by

*To whom correspondence should be addressed. E-mail: hpyou@ciac.jl.cn.

(1) Feldmann, C.; Jüstel, T.; Ronda, C. R.; Schmidt, P. J. *Adv. Funct. Mater.* **2003**, *13*, 511.
(2) Höppe, H. A. *Angew. Chem., Int. Ed.* **2009**, *48*, 3572.
(3) Xie, R. J.; Hirosaki, N.; Suehiro, T.; Xu, F. F.; Mitomo, M. *Chem. Mater.* **2006**, *18*, 5518.
(4) Tang, Y. S.; Hu, S. F.; Ke, W. C.; Lin, C. C.; Bagkar, N. C.; Liu, R. S. *Appl. Phys. Lett.* **2008**, *93*, 131114.
(5) Song, Y. H.; Jia, G.; Yang, M.; Huang, Y. J.; You, H. P.; Zhang, H. J. *Appl. Phys. Lett.* **2009**, *94*, 091902.
(6) Chang, C. K.; Chen, T. M. *Appl. Phys. Lett.* **2007**, *90*, 161901.
(7) Shur, M. S.; Zukauskas, A. *Proc. IEEE* **2005**, *93*, 1691.
(8) Piao, X. Q.; Horikawa, T.; Hanzawa, H.; Machida, K. *Appl. Phys. Lett.* **2006**, *88*, 161908.
(9) Mazzeo, M.; Vitale, V.; Della Sala, F.; Anni, M.; Barbarella, G.; Favaretto, L.; Sotgiu, G.; Cingolani, R.; Gigli, G. *Adv. Mater.* **2005**, *17*, 34.
(10) Liu, Y.; Nishiura, M.; Wang, Y.; Hou, Z. M. *J. Am. Chem. Soc.* **2006**, *128*, 5592.
(11) Yao, G. Q.; Lin, J. H.; Zhang, L.; Lu, G. X.; Gong, M. L.; Su, M. Z. *J. Mater. Chem.* **1998**, *8*, 585.


Published on Web 11/02/2010

codoping $Eu^{2+}$ and $Mn^{2+}$ ions under effective resonance-type energy transfer in a single-phased host. Therefore, a single-phased white-light-emitting phosphor based on the mechanism of energy transfer has been realized by doping coactivators in some host lattices such as $CaAl_2Si_2O_8$:Eu,Mn,[12] $Ba_3MgSi_2O_8$:Eu,Mn,[13] $Ca_{10}K(PO_4)_7$:Eu,Mn,[14] $\alpha$-$Sr(PO_3)_2$:Eu,Mn,[15] and $Ca_3Mg_3(PO_4)_4$:Eu,Mn.[16] However, to the best of our knowledge, the luminescent properties and energy transfer of $Eu^{2+}$ and $Mn^{2+}$ in a $Ca_9Lu(PO_4)_7$ host have not been reported.

$\beta$-$Ca_3(PO_4)_2$ (space group $R3c$, $Z = 21$) is isostructural to the natural mineral whitlockite. This special crystal structure permits rich heterovalent substitution of $Ca^{2+}$ by $M^+$ (monovalent), $R^{3+}$ (trivalent), and $R^{4+}$ (quadrivalent) cations. These different substitutions in the initial $\beta$-$Ca_3(PO_4)_2$ can create many kinds of materials with a $\beta$-$Ca_3(PO_4)_2$-type structure, which preserve a polar whitlockite-type crystal structure, and have served as the base for the crystallochemical design of compounds with nonlinear-optical, catalytic, ferroelectric, and ion-conductive properties.[17] Lazoryak et al.[18] have investigated the reduction and reoxidation behavior of $Ca_9Fe(PO_4)_7$, which has potential applications as a catalyst, a material for cleaning gas mixtures from hydrogen, and a material intermediator for two-stage hydrogen oxidation. However, the luminescent property of this kind of phosphate was rarely reported.[19]

In this paper, we describe the synthesis and luminescence of a novel white-light-emitting $Ca_9Lu(PO_4)_7$:$Eu^{2+}$,$Mn^{2+}$ phosphor suitable for use in a UV LED. The strong excitation band of the phosphor in the wavelength range of 250−430 nm has favorable properties for application as a LED conversion phosphor. We also investigate its luminescence properties as well as the energy-transfer phenomenon between the sensitizer and activator.

## 2. Experimental Section

**2.1. Materials and Synthesis.** Powder samples $Ca_{9(1-m-n)}Lu(PO_4)_7$:$mEu^{2+}$,$nMn^{2+}$ (CLuP:$mEu^{2+}$,$nMn^{2+}$) have been prepared by a solid-state reaction method. The raw materials were $CaCO_3$ [analytical reagent (A.R.)], $NH_4H_2PO_4$ (A.R.), $Lu_2O_3$ (99.99%), $Eu_2O_3$ (99.99%), and $MnCO_3$ (A.R.). The stoichiometric amount of raw materials was thoroughly mixed by grinding in an agate mortar. They were then put into crucibles and subsequently heated at 1473 K for 4 h in a CO atmosphere. After regrinding, they were sintered at 1473 K under a 10% $H_2$−90% $N_2$ gas mixture for 2 h. Finally, the as-synthesized samples were slowly cooled to room temperature inside the tube furnace under a $H_2$−$N_2$ flow.

**2.2. Measurements and Characterization.** Powder X-ray diffraction (XRD) measurements were performed on a D8 focus diffractometer (Bruker) at a scanning rate of 0.2°/min in the $2\theta$ range from 10° to 70°, with graphite-monochromatized Cu K$\alpha$ radiation ($\lambda$ = 0.154 05 nm) operating at 40 kV and 40 mA. Field-emission scanning electron microscopy (FE-SEM) images were taken on S-4800 (Hitachi Co.) electron microscopes. The photoluminescence (PL) and PL excitation (PLE) spectra of the obtained powders were recorded with a Hitachi F-4500 spectrophotometer equipped with a 150 W xenon lamp as the excitation source. The diffuse-reflectance spectra were obtained by a Hitachi U-4100 spectrophotometer with the reflection of black felt (reflection 3%) and white $Al_2O_3$ (reflection 100%) in the wavelength region of 200−600 nm. The luminescence decay curve was obtained from a Lecroy Wave Runner 6100 digital oscilloscope (1 GHz) using a tunable laser (pulse width = 4 ns; gate = 50 ns) as the excitation source (Continuum Sunlite OPO). All of the measurements were performed at room temperature.

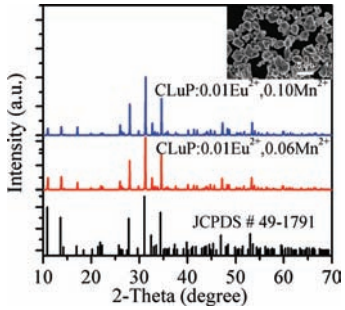


**Figure 1.** XRD patterns of CLuP:0.01$Eu^{2+}$,0.06$Mn^{2+}$ and CLuP:0.01-$Eu^{2+}$,0.10$Mn^{2+}$ samples. The standard data for $Ca_9Lu(PO_4)_7$ (JCPDS card no. 49-1791) are shown as reference. The inset shows an FE-SEM micrograph of the CLuP:0.01$Eu^{2+}$,0.05$Mn^{2+}$ sample.

## 3. Results and Discussion

**3.1. Phase Identification and Morphology.** Figure 1 presents the representative XRD patterns of the CLuP:0.01$Eu^{2+}$,0.06$Mn^{2+}$ and CLuP:0.01$Eu^{2+}$,0.10$Mn^{2+}$ samples. All of the diffraction peaks of the samples can be basically indexed to the standard data of $Ca_9Lu(PO_4)_7$ (JCPDS card no. 49-1791). No other phase is detected, indicating that the obtained samples are single phase and the $Eu^{2+}$ and $Mn^{2+}$ ions have been successfully incorporated in the $Ca_9Lu(PO_4)_7$ host lattices by replacing $Ca^{2+}$ due to their similar ionic radii and charge.[20] $Ca_9Lu(PO_4)_7$ is related to the mineral whitlockite and is isostructural with the $\beta$-$Ca_3(PO_4)_2$ structure. Compound $\beta$-$Ca_3(PO_4)_2$ has six metal sites, M1−M6. The M1, M2, and M3 sites are eight-coordinated by oxygen atoms, the M4 site, surrounded by nine oxygen atoms, is 50% occupied by $Ca^{2+}$ ions, the distorted octahedral M5 site is fully occupied by $Ca^{2+}$ ions, and the M6 site is vacant.[21] In the structure of $Ca_9Lu(PO_4)_7$, $Lu^{3+}$ cations statistically occupy the M1, M2, and M5 positions of the $\beta$-$Ca_3(PO_4)_2$ structure together with $Ca^{2+}$ ions, and the cationic positions M4 and M6 are completely empty.[22] The inset in Figure 1 shows the FE-SEM micrograph of the CLuP:0.01$Eu^{2+}$,0.05$Mn^{2+}$ samples. It is clearly seen that the samples are composed of aggregated particles with size ranging from 0.5 to 5 $\mu$m, which is acceptable for the white-light LED application.

(12) Yang, W. J.; Luo, L.; Chen, T. M.; Wang, N. S. *Chem. Mater.* **2005**, *17*, 3883.
(13) Kim, J. S.; Jeon, P. E.; Choi, J. C.; Park, H. L.; Mho, S. I.; Kim, G. C. *Appl. Phys. Lett.* **2004**, *84*, 2931.
(14) Liu, W. R.; Chiu, Y. C.; Yeh, Y. T.; Jang, S. M.; Chen, T. M. *J. Electrochem. Soc.* **2009**, *156*, J165.
(15) Höppe, H. A.; Daub, M.; Bröhmer, M. C. *Chem. Mater.* **2007**, *19*, 6358.
(16) Kwon, K. H.; Im, W. B.; Jang, H. S.; Yoo, H. S.; Jeon, D. Y. *Inorg. Chem.* **2009**, *48*, 11525.
(17) Belik, A. A.; Yanov, O. V.; Lazoryak, B. I. *Mater. Res. Bull.* **2001**, *36*, 1863.
(18) Lazoryak, B. I.; Belik, A. A.; Kotov, R. N.; Leonidov, I. A.; Mitberg, E. B.; Karelina, V. V.; Kellerman, D. G.; Stefanovich, S. Y.; Avetisov, A. K. *Chem. Mater.* **2003**, *15*, 625.
(19) Huang, Y. L.; Jiang, C. F.; Cao, Y. G.; Shi, L. A.; Seo, H. J. *Mater. Res. Bull.* **2009**, *44*, 793.
(20) Shannon, R. D. *Acta Crystallogr., Sect. A* **1976**, *32*, 751.
(21) Belik, A. A.; Izumi, F.; Ikeda, T.; Okui, M.; Malakho, A. P.; Morozov, V. A.; Lazoryak, B. I. *J. Solid State Chem.* **2002**, *168*, 237.
(22) Golubev, V. N.; Lazoryak, B. I. *Inorg. Mater.* **1991**, *27*, 480.

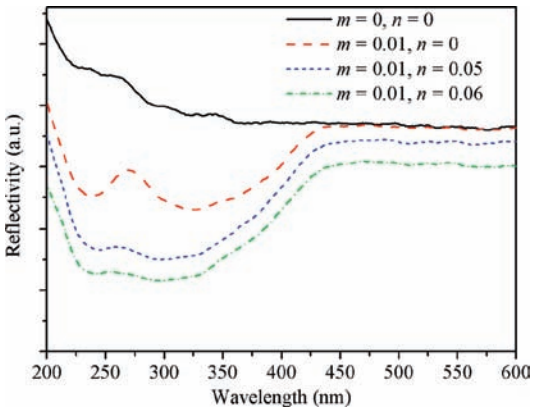


**Figure 2.** Diffuse-reflectance spectra of CLuP:$m$Eu$^{2+}$,$n$Mn$^{2+}$ samples.

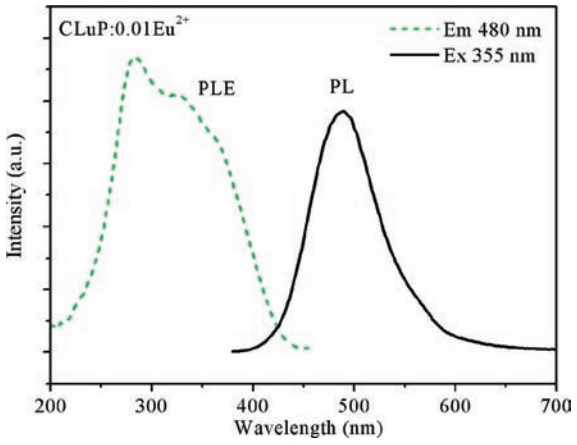


**Figure 3.** PLE and PL spectra of the CLuP:Eu$^{2+}$ phosphor.

**3.2. Luminescence properties.** The UV−visible absorption features of the CLuP, CLuP:Eu$^{2+}$, and CLuP:Eu$^{2+}$, Mn$^{2+}$ samples were investigated by the diffuse-reflectance spectra. As shown in Figure 2, the spectrum of the CLuP host exhibits a high reflection in the visible range. The CLuP:Eu$^{2+}$ samples display strong absorption bands between 230 and 430 nm attributed to the 4f$^7$−4f$^6$5d$^1$ electronic transition absorption of the Eu$^{2+}$ ions. For the Eu$^{2+}$- and Mn$^{2+}$-codoped CLuP samples, they also show a strong absorption band in the wavelength range of 230−430 nm except for the enhanced absorption intensity by Mn$^{2+}$ ions,[23] indicating that the doubly doped phosphor may be suitable for UV LED excitation.

Figure 3 illustrates the PLE and PL spectra of CLuP:Eu$^{2+}$. Upon excitation of 355 nm, the CLuP:0.01Eu$^{2+}$ phosphor exhibits an intense blue-green luminescence, and the corresponding emission spectrum consists of a broad blue-green emission band around 480 nm due to the electric-dipole-allowed transition from the lowest level of the 5d excited state to the 4f ground state of the Eu$^{2+}$ ions. In our case, the value of the full width at half-maximum (fwhm) is about 85 nm. The value of the fwhm is bigger than that of the common value (~70 nm) in most phosphor materials, which is due to the different luminescent centers in the host material. In the illumination application field, the bigger fwhm of the emission band is helpful for high color rendering indexes. Monitored by the emission at 480 nm, the PLE spectrum shows an unresolved broad band from 230 to 430 nm, which is assigned to the transition between the ground-state 4f$^7$ and the crystal-field split 4f$^6$5d configuration. The dominant bands in the PLE spectrum are difficult to resolve because of the 4f5d multiplet excited states of the Eu$^{2+}$ ions and the serious overlap between 5d levels. The samples presented a blue-green emission band peaking at 480 nm and an excitation subband centered at 368 nm, so the Stokes shift of the CLuP:0.01Eu$^{2+}$ phosphor is estimated to be about 6300 cm$^{-1}$.

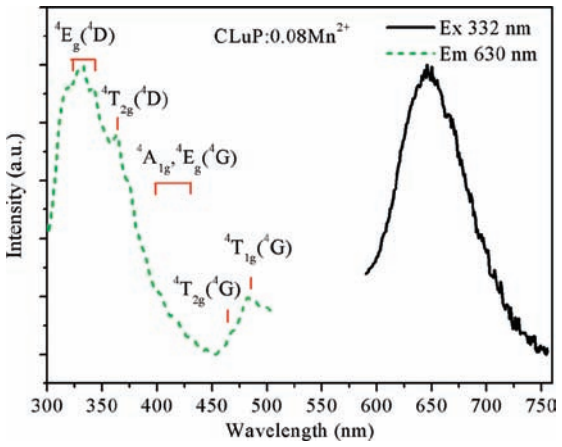


**Figure 4.** PLE and PL spectra of the CLuP:Mn$^{2+}$ phosphor.

Figure 4 shows the PL and PLE spectra of the Mn$^{2+}$-doped CLuP phosphor. The PLE spectrum consists of several weak bands in the UV and visible regions. These bands are assigned to the spin-forbidden transitions in the 3d$^5$ electron configuration of the Mn$^{2+}$ ions. On the basis of the Orgel diagram for divalent manganese,[24] the two bands centered at 332 and 343 nm are components of the $^4$E($^4$D) levels, and the bands in the region from 400 to 430 nm are the splitting of $^4$E−$^4$A$_1$($^4$G) levels. The other bands peaking at about 364, 465, and 483 nm are attributed to transitions of the Mn$^{2+}$ ions from the ground-state level $^6$A$_1$($^6$S) to $^4$T$_2$($^4$D), $^4$T$_2$($^4$G), and $^4$T$_1$($^4$G) excited-state levels, respectively. Because the d−d transitions of the Mn$^{2+}$ ion are spin- and parity-forbidden by the selection rules, the intensity of these absorptions is low in the UV region. The PL spectrum of CLuP:Mn$^{2+}$ exhibits a broad red emission band from 580 to 750 nm centered at 645 nm ascribed to the spin-forbidden $^4$T$_1$($^4$G) → $^6$A$_1$($^6$S) transition of the Mn$^{2+}$ ions. Mn$^{2+}$-doped luminescent materials have been known to show wide-ranging emission from 500 to 700 nm, which is strongly affected by the strength of the crystal field and coordination number. The stronger the crystal field, the longer the emission position will be.[25] At the same time, the coordination number also has a great effect on the emission color. Tetrahedrally coordinated Mn$^{2+}$ in the host usually gives a green to yellow emission, whereas it emits red light in octahedral coordination.[11,25] In our case, the phosphors emit a broad red emission band peaked at 645 nm. Therefore, it is reasonable to propose that the Mn$^{2+}$ ions prefer to occupy the Ca$^{2+}$ sites with octahedral coordination in the host lattice.

(23) Wang, J.; Wang, S. B.; Su, Q. *J. Mater. Chem.* **2004**, *14*, 2569.
(24) Orgel, L. E. *J. Chem. Phys.* **1955**, *23*, 1004.
(25) Shi, L. A.; Huang, Y. L.; Seo, H. J. *J. Phys. Chem. A* **2010**, *114*, 6927.

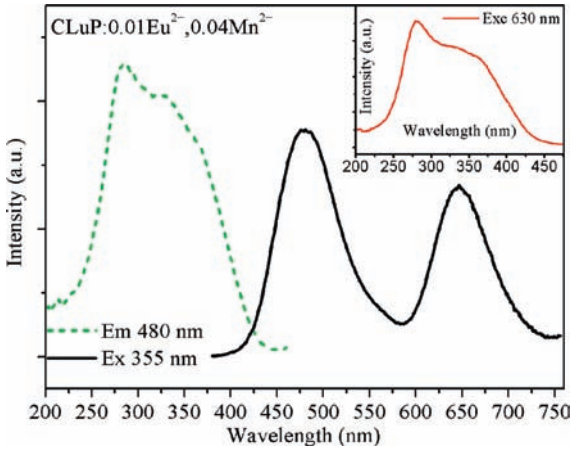


**Figure 5.** PLE and PL spectra of the CLuP:$Eu^{2+}$, $Mn^{2+}$ phosphor.

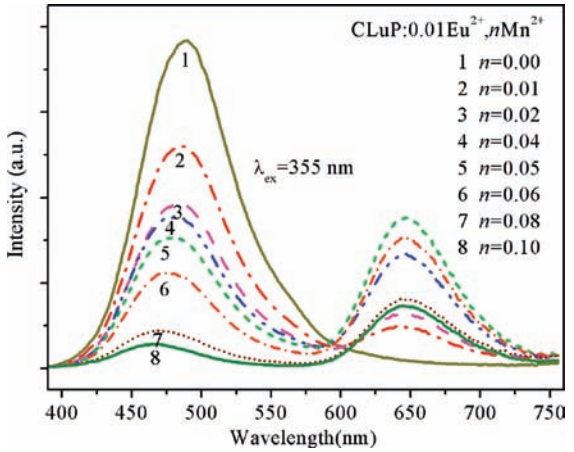


**Figure 6.** PL spectra for CLuP:0.01$Eu^{2+}$,$n$$Mn^{2+}$ phosphors on the $Mn^{2+}$ doping content ($n$).

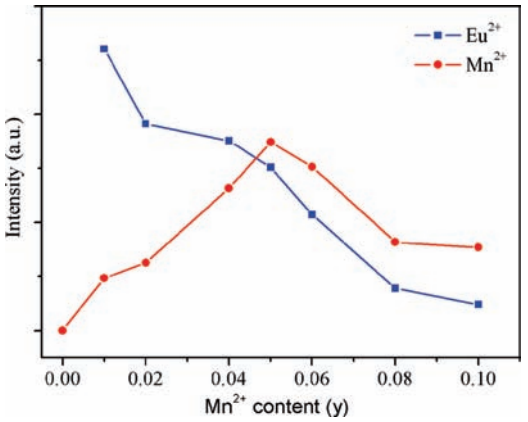


**Figure 7.** Dependence of the relative emission intensity of $Eu^{2+}$ and $Mn^{2+}$ for CLuP phosphors on the $Mn^{2+}$ content ($n$).

One of the essential conditions usually required for energy transfer is the overlap between the donor emission and the acceptor excitation spectra. Comparing the emission spectrum of CLuP:$Eu^{2+}$ with the excitation spectrum of CLuP:$Mn^{2+}$, one can find a significant spectral overlap between the emission band of the $Eu^{2+}$ ions and the excitation band of the $Mn^{2+}$ ions. Therefore, it can be speculated that energy transfer from the $Eu^{2+}$ to $Mn^{2+}$ ions may occur. Figure 5 shows the PL and PLE spectra of the $Eu^{2+}$- and $Mn^{2+}$-coactivated CLuP phosphor. The PLE spectrum (inset in Figure 5) monitored by the $Mn^{2+}$ emission has a profile similar to that of the excitation band monitored by the $Eu^{2+}$ emission, revealing that the $Mn^{2+}$ ions are essentially excited through the $Eu^{2+}$ ions. This result demonstrates that an efficient energy transfer from the $Eu^{2+}$ to $Mn^{2+}$ ions occurs. The PLE spectrum of the $Mn^{2+}$ ions in the $Eu^{2+}$- and $Mn^{2+}$-coactivated sample extends from 230 to 430 nm, indicating that this phosphor could be used in a UV white-light LED. Upon excitation of 355 nm, the PL spectrum of CLuP:$Eu^{2+}$,$Mn^{2+}$ consists of a broad blue-green band and a red emission band (Figure 5). The broad blue-green emission band from 400 to 580 nm is characteristic of the allowed f−d transition of the $Eu^{2+}$ ions, whereas the intense red emission centered at 645 nm is attributed to the $^4T_1-{}^6A_1$ forbidden transition of the $Mn^{2+}$ ions. The emission spectrum nearly covers the entire visible region. Therefore, the relative intensities of these two emissions can be varied and further combined to form pure white light in a single host lattice by simply adjusting the amounts of the activators through the principle of energy transfer. It is believed that the obtained white light would enable easy fabrication with perfect stability and color reproducibility.

In order to optimize the white-light-emitting performance of the phosphors, a series of samples with nominal compositions of CLuP:0.01$Eu^{2+}$,$n$$Mn^{2+}$ (from $n = 0$ to 0.10) were synthesized and their luminescent properties systematically investigated. Figure 6 shows the PL spectra of the CLuP:0.01$Eu^{2+}$,$n$$Mn^{2+}$ phosphors with different doping contents $n$, which were observed at an excitation wavelength of 355 nm. The intensity of the $Eu^{2+}$ emission was found to decrease monotonically with an increase in the $Mn^{2+}$ content, whereas the emission intensity of the $Mn^{2+}$ ions reaches a maximum at $n = 0.05$ and then begins to decrease as a result of the concentration quenching of the $Mn^{2+}$ ions (Figure 7). These results indicate that the efficient energy transfer from the $Eu^{2+}$ to $Mn^{2+}$ ions.

In order to well understand the energy-transfer process, we measured the PL decay curves and then calculated the lifetimes as well as energy-transfer efficiencies. Figure 8 shows the PL decay curves of the $Eu^{2+}$ ions in CLuP:0.01$Eu^{2+}$,$n$$Mn^{2+}$, which were measured with excitation at 355 nm and monitored at 480 nm. One can see that the decay curve of the singly $Eu^{2+}$-doped CLuP sample can be well fitted into a single-exponential function with a decay time of 0.83 $\mu$s. This is the radiative decay time of the $Eu^{2+}$ ions. For the $Eu^{2+}$- and $Mn^{2+}$-codoped samples, the doping of the $Mn^{2+}$ ions significantly modifies the fluorescent dynamics of the $Eu^{2+}$ ions. The results reveal that the fluorescence decays deviate slightly from a single-exponential rule, indicating the presence of a nonradiative process. The effective lifetime is defined as

$$\tau = \frac{\int_0^\infty tI(t)\,dt}{\int_0^\infty I(t)\,dt} \quad (1)$$

On the basis of eq 1, the effective lifetime values were calculated to be 0.75, 0.66, 0.61, 0.54, 0.49, 0.38, and 0.14 $\mu$s for CLuP:0.01$Eu^{2+}$,$n$$Mn^{2+}$ with $n = 0.01$, 0.02, 0.04, 0.05, 0.06, 0.08, and 0.10, respectively. It can be seen that the decay lifetime of the $Eu^{2+}$ ions decreases monotonically

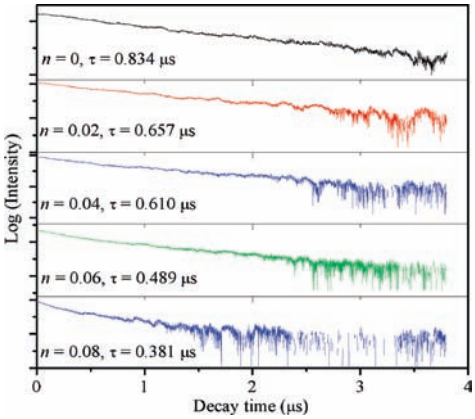


**Figure 8.** PL decay curves of $Eu^{2+}$ in CLuP:0.01$Eu^{2+}$,*n*$Mn^{2+}$ (excited at 355 nm and monitored at 480 nm).

with an increase in the $Mn^{2+}$ doping concentration, which strongly supports energy transfer from the $Eu^{2+}$ to $Mn^{2+}$ ions, and the energy-transfer process may happen via resonant-type mechanism.[5,26]

The energy-transfer efficiency ($\eta_T$) from the $Eu^{2+}$ to $Mn^{2+}$ ions in the CLuP:0.01$Eu^{2+}$,*n*$Mn^{2+}$ phosphors was calculated by using the formula[27]

$$\eta_T = 1 - \tau_S/\tau_{S_0} \quad (2)$$

where $\tau_{S_0}$ is the radiative decay lifetime of the $Eu^{2+}$ ions and $\tau_S$ is the lifetime of the $Eu^{2+}$ ions in the presence of the $Mn^{2+}$ ions. The decay lifetime values were used for calculation, and the results are presented in Figure 9. The energy-transfer efficiency was found to increase gradually from $n = 0$ to 0.10 with an increase of the $Mn^{2+}$ concentration.

The resonant energy-transfer mechanism consists of two types: one is exchange interaction and another is multipolar interaction.[28,29] It is known that if energy transfer takes the exchange interaction, the critical distance between the sensitizer and activator should be shorter than 3−4 Å.[29] The critical distance $R_C$ for energy transfer from the $Eu^{2+}$ to $Mn^{2+}$ ions was calculated using the concentration-quenching method. The critical distance was estimated according to the following equation:[30]

$$R_C \approx 2\left[\frac{3V}{4\pi x_C N}\right]^{1/3} \quad (3)$$

Here $V$ is the volume of the unit cell, $x_C$ is the critical concentration, and $N$ is the number of available sites for the dopant in the unit cell. In our case, $N$ is 6, and $V$ is estimated to be 3518.37 $Å^3$ with the assumption that the lattice parameters are almost constant with $Eu^{2+}$ and $Mn^{2+}$ doping levels. The critical concentration is about 0.75 from the total concentration of the $Eu^{2+}$ and $Mn^{2+}$ ions at which the energy-transfer efficiency is 0.5. From the above equation, the critical distance $R_C$ was calculated to be

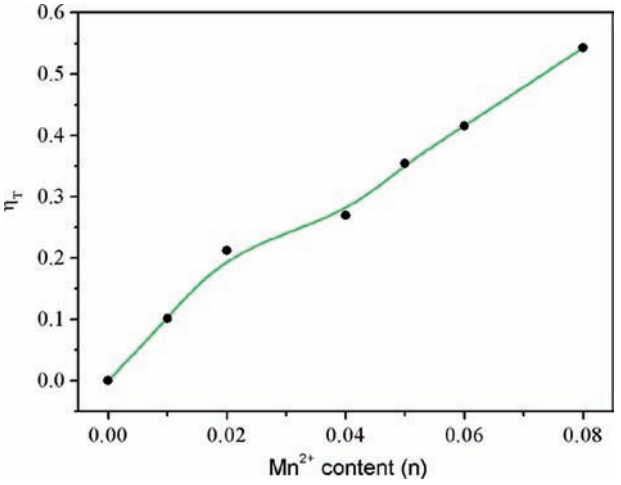


**Figure 9.** Dependence of the energy-transfer efficiency $\eta_T$ on the $Mn^{2+}$ content (*n*).

about 11.4 Å. This value is longer than 3−4 Å, indicating little possibility of energy transfer via the exchange interaction mechanism. Thus, the electric multipolar interaction can take place for energy transfer between the $Eu^{2+}$ and $Mn^{2+}$ ions.

According to Dexter's energy-transfer expressions of multipolar interaction and Reisfeld's approximation, the following relation can be given:[28,30,31]

$$\frac{\tau_{S_0}}{\tau_S} \propto C^{n/3} \quad (4)$$

where $n = 6$, 8, and 10 are dipole−dipole, dipole−quadrupole, and quadrupole−quadrupole interactions, respectively. $C$ is the doping concentration of the $Mn^{2+}$ ions. The $\tau_{S_0}/\tau_S$−$C^{n/3}$ plots are further illustrated in Figure 10a−c, and the relationships are observed when $n = 6$, 8, and 10. A linear relationship was observed when $n = 8$. This clearly indicates that the energy-transfer mechanism from the $Eu^{2+}$ to $Mn^{2+}$ ions is a dipole−quadrupole reaction. Therefore, the electric dipole−quadrupole interaction predominates in the energy-transfer mechanism from the $Eu^{2+}$ to $Mn^{2+}$ ions in CLuP. Considering the dipole−quadrupole interaction, the critical distance from a sensitizer to an acceptor is given by the spectral overlap method. Hence, $R_C$ can be obtained from the formula[32]

$$R_C{}^8 = 3.024 \times 10^{12} \lambda_S{}^2 f_q \int \frac{F_S(E)\, F_A(E)\, dE}{E^4} \quad (5)$$

where $f_q$ is the oscillator strength of the involved absorption transition of the acceptor ($Mn^{2+}$), $\lambda_S$ (in angstroms) is the wavelength position of the sensitizer's emission, $E$ is the energy involved in the transfer (in electronvolts), and $\int F_S(E)\, F_A(E)\, dE/E^4$ represents the spectral overlap between the normalized shapes of the $Eu^{2+}$ emission $F_S(E)$ and the $Mn^{2+}$ excitation $F_A(E)$, and in our case. it is calculated to be about 0.023 56 $eV^{-5}$. Using the above equation with $f_q = 10^{-10}$, the critical distance $R_C$ was estimated to be 10.7 Å, which agrees approximately with

(26) Jiao, H.; Liao, F.; Tian, S.; Jing, X. *J. Electrochem. Soc.* **2003**, *150*, H220.
(27) Paulose, P. I.; Jose, G.; Thomas, V.; Unnikrishnan, N. V.; Warrier, M. K. R. *J. Phys. Chem. Solids* **2003**, *64*, 841.
(28) Reisfeld, R.; Greenberg, E.; Velapoldi, R.; Barnett, B. *J. Chem. Phys.* **1972**, *56*, 1698.
(29) Antipeuko, B. M.; Bataev, I. M.; Ermolaev, V. L.; Lyubimov, E. I.; Privalova, T. A. *Opt. Spectrosc.* **1970**, *29*, 177.
(30) Blasse, G. *Philips Res. Rep.* **1969**, *24*, 131.
(31) Dexter, D. L.; Schulman, J. A. *J. Chem. Phys.* **1954**, *22*, 1063.
(32) You, H. P.; Zhang, J. L.; Hong, G. Y.; Zhang, H. J. *J. Phys. Chem. C* **2007**, *111*, 10657.

that obtained by using the concentration-quenching method. This result further reveals that the mechanism of energy transfer from the $Eu^{2+}$ to $Mn^{2+}$ ions is mainly due to a dipole−quadrupole interaction.

The excited-state donor ions can relax by direct energy transfer to acceptor ions or after migration of the excitation among donor ions until an acceptor is reached. If the migration process among donors is negligible versus the energy-transfer donor−acceptor, then the temporal evolution of the donor popular after a pulsed excitation follows the Inokuti−Hirayama (I−H) model,[33] and the fluorescence decay intensity $I(t)$ is given by

$$I(t) = I(0)\exp\left[-\frac{t}{\tau_0} - Qt^{3/S}\right] \quad (6)$$

where $\tau_0$ is the donor lifetime in the absence of acceptors and the value of $S = 6$, 8, or 10 corresponds to the dominant mechanism being the dipole−dipole, dipole−quadrupole, or quadrupole−quadrupole interaction, respectively. The energy-transfer parameter $Q$ is defined as

$$Q = \frac{4\pi}{3} C_A \Gamma\left(1 - \frac{3}{S}\right)[C_{DA}^{(S)}]^{3/S} \quad (7)$$

where $C_A$ is the concentration of acceptors, $\Gamma(x)$ is the gamma function, and $C_{DA}^{(S)}$ is the microscopic energy-transfer parameter that characterizes the process.

However, if the migration process among donors is important, the problem is more complex and different approximations have been developed to analyze this situation. One possibility is to consider the energy migration as a diffusion process. This method was adopted by Yokota and Tanimoto (Y−T),[34] who obtained an expression for the temporal evolution of excited-state donors considering strong dipole−dipole interaction between donors and acceptors with weak diffusion. In order to take the high-order mechanism into account, Martín et al.[35] proposed a generalization of the Y−T expression for any kind of multipolar interaction. The expression for the temporal evolution of the donor luminescent signal is given by

$$I(t) = I(0)\exp\left[-\frac{t}{\tau_0} - Qt^{3/S}\left(\frac{1 + a_1X + a_2X^2}{1 + b_1X}\right)^{S-3/S-2}\right] \quad (8)$$

where $a_1$, $a_2$, and $b_1$ are the approximant coefficients that depend on the multipolar character of the interaction and

$$X = D[C_{DA}^{(S)}]^{-2/S}t^{1-2/S} \quad (9)$$

where $D$ is the diffusion coefficient that characterizes the energy-transfer processes between donors. In order to characterize the Eu−Mn energy-transfer processes, the luminescence decay curves have been fitted using the generalized Y−T (eq 8) and I−H (eq 6) models. The decay curves of luminescence and theoretical fit were presented in Figures S1−S3 (Supporting Information). The best fit was obtained in the I−H model ($S = 8$, no migration). It is indicated that the dominant interaction of the energy transfer between the $Eu^{2+}$ and $Mn^{2+}$ ions can be determined as the dipole−quadrupole interaction not involving the migration in the present case.

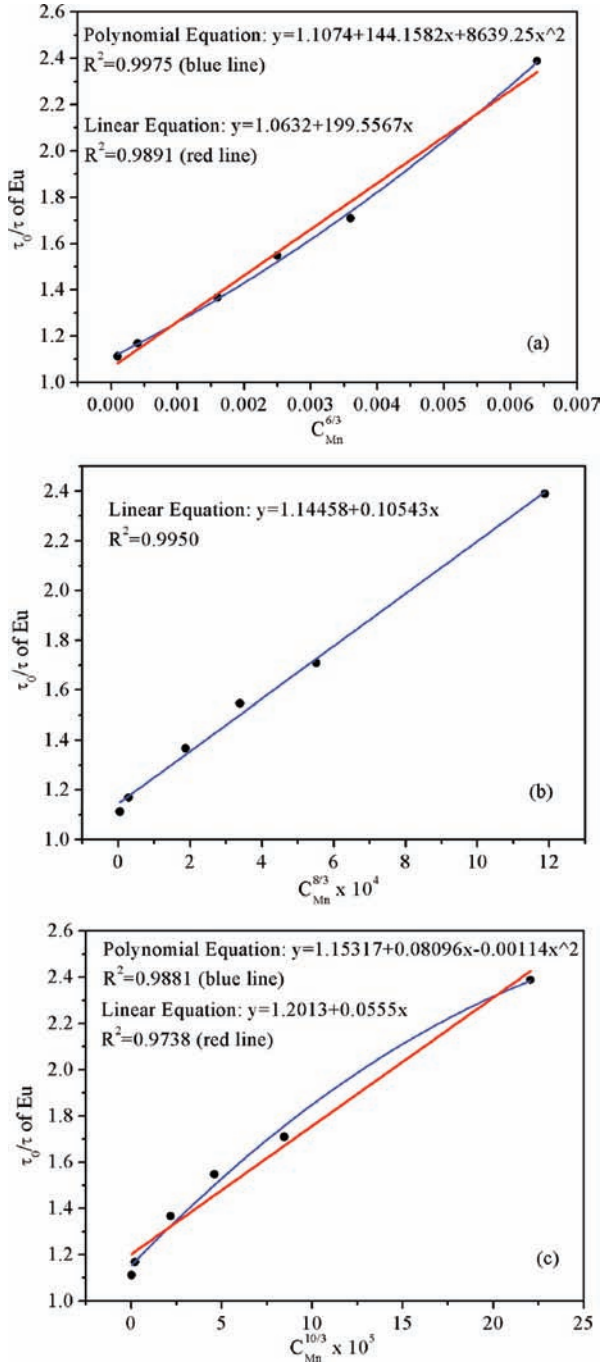


**Figure 10.** Dependence of $\tau_0/\tau$ of $Eu^{2+}$ on (a) $C^{6/3}$, (b) $C^{8/3}$, and (c) $C^{10/3}$.

The Commission Internationale de L'Eclairage (CIE) chromaticity coordinates and correlated color temperature (CCT) of the CLuP:0.01$Eu^{2+}$,$n$$Mn^{2+}$ phosphors with different doping contents of $Mn^{2+}$ are summarized in Table 1. The chromaticity coordinates were calculated based on the corresponding PL spectrum, and they are

(33) Inokuti, M.; Hirayama, F. *J. Chem. Phys.* **1965**, *43*, 1978.
(34) Yokota, M.; Tanimoto, O. *J. Phys. Soc. Jpn.* **1967**, *22*, 779.
(35) Martín, I. R.; Rodríguez, V. D.; Rodríguez-Mendoza, U. R.; Lavín, V. *J. Chem. Phys.* **1999**, *111*, 1191.

**Table 1.** Comparison of the CIE Chromaticity Coordinates ($x$, $y$) and CCT ($T_C$) for CLuP:0.01$Eu^{2+}$,$nMn^{2+}$ Phosphors Excited at 355 nm

| sample no. | sample composition ($n$) | CIE coordinates ($x$, $y$) | CCT ($T_C$) |
|---|---|---|---|
| A | 0 | (0.172, 0.316) | 20194 |
| B | 0.01 | (0.200, 0.297) | 19463 |
| C | 0.02 | (0.221, 0.287) | 17348 |
| D | 0.04 | (0.274, 0.280) | 11205 |
| E | 0.05 | (0.315, 0.278) | 6904 |
| F | 0.06 | (0.333, 0.268) | 5431 |
| G | 0.08 | (0.367, 0.248) | 2715 |
| H | 0.10 | (0.416, 0.240) | 1903 |

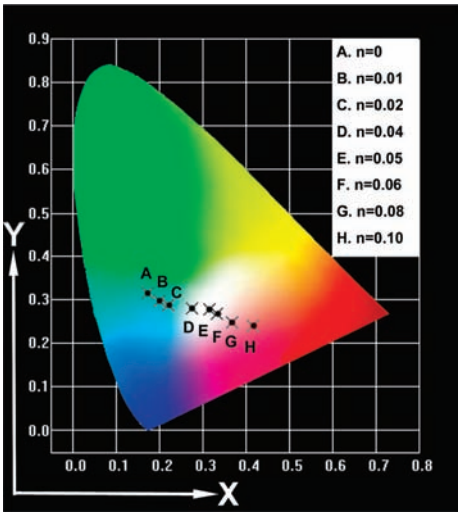


**Figure 11.** CIE chromaticity diagram for CLuP:0.01$Eu^{2+}$,$nMn^{2+}$ phosphors excited at 355 nm: (A) $n = 0$, (B) $n = 0.02$, (C) $n = 0.04$, (D) $n = 0.05$, (E) $n = 0.06$, (F) $n = 0.08$, (G) $n = 0.10$.

also represented in Figure 11. The CCT was calculated by using McCamy's approximate formula.[36] Energy transfer makes it possible to obtain both the blue-green emission of the $Eu^{2+}$ ions and the red emission of the $Mn^{2+}$ ions in a single host, which is the basis for generating white light under excitation of UV light. As shown in Figure 11, one can find that the color tone of the phosphors shifts gradually from blue-green to white and eventually to red with an increase in the doping content of the $Mn^{2+}$ions, confirming that the CIE chromaticity coordinates are tunable through adjustment of the content of the $Mn^{2+}$ ions. Therefore, the white light with a desired CCT can be obtained through simple control of the doping $Mn^{2+}$ content to meet the needs of different illumination applications.

(36) McCamy, C. S. *Color Res. Appl.* **1992**, *17*, 142.

## 4. Conclusion

In summary, a color-tunable single-phased CLuP:$Eu^{2+}$, $Mn^{2+}$ phosphor was developed for the first time. The emission color of the obtained phosphors can be easily modulated from blue-green to white and eventually to red by simply adjusting the amount of $Mn^{2+}$ because of the different emission compositions of the $Eu^{2+}$ and $Mn^{2+}$ ions. The fluorescence decay dynamics and luminescent properties of the CLuP:$Eu^{2+}$,$Mn^{2+}$ phosphor confirm the efficient energy transfer from the $Eu^{2+}$ to $Mn^{2+}$ ions. Analysis reveals that the dipole−quadrupole reaction should be responsible for energy transfer from the $Eu^{2+}$ to $Mn^{2+}$ ions. The critical distance of the $Eu^{2+}$ and $Mn^{2+}$ ions has also been calculated. Because the phosphor exhibits a strong absorption in the range of the near-UV spectral region and white-light emission, it may serve as a potential white-light-emitting UV-convertible phosphor in white-light LED devices.

**Acknowledgment.** This work is financially supported by the National Natural Science Foundation of China (Grant 20771098), the Fund for Creative Research Groups (Grant 20921002), and the National Basic Research Program of China (973 Program, Grant 2007CB935502).

**Supporting Information Available:** PL decay curves of $Eu^{2+}$ in CLuP:0.01$Eu^{2+}$,$nMn^{2+}$ (excited at 355 nm and monitored at 480 nm), with solid lines corresponding to fits to the I−H model (Figures S1 and S2), and PL decay curves of $Eu^{2+}$ in CLuP:0.01$Eu^{2+}$,$nMn^{2+}$, with solid lines corresponding to fits to the generalized Y−T diffusion model (Figure S3). This material is available free of charge via the Internet at http://pubs.acs.org.